(Received 24 January 2024, Accepted 28 February 2024, Scheduled 6 March 2024)

Analysis of a Compact Dual/Single Band Tunable BPF for 5G/X-Band Applications

Surendra B. Velagaleti[1, 2, *] and Siddaiah Nalluri[1]

[1]*Department of Electronics and Communication Engineering, Koneru Lakshmaiah Education Foundation Vaddeswaram, Guntur District, India*
[2]*Department of Electronics and Communication Engineering, C. R. Reddy Engineering College, Eluru, India*

ABSTRACT: Currently, various microwave filter designs contend for the use in wireless communications. Among several microstrip filter designs, the tunable filter presents more advantages and better prospects for wireless communication applications, being compact in size, cost effective, and light in weight. These reconfigurable microwave filters can reduce the number of switches between the electronic components. The number of switches among the electronic devices can be decreased using tunable BPF. The tunable BPF is designed for X-band satellite communication applications as well as n77, n78, and n79 5G applications, and HSCH 3486 PIN diode is used to achieve the filter's tunability. An impedance bandwidth of 2.4 GHz and 2 GHz (fractional bandwidth of 25%) has been achieved with an S_{21} less than -1.5 dB, -2 dB and S_{11} of -22 dB and -31 dB at both the resonating frequencies. Semicircular cavity bandpass filter has been designed with the center frequency of 3.7 GHz. Switching between the two passbands has been obtained by attaching a PIN diode between the input and output feed lines.

1. INTRODUCTION

The 3GPP developed the new radio (NR) for the fifth generation (5G) of cellular networks, which is a new Radio Access Technology (RAT) for the 5G mobile network. It was intended to serve as the worldwide standard for 5G networks' air interface. n77, n78, n79, and 5G Wi-Fi, which comprise the US' 3.3 to 4.2 GHz 5G band, Japan's 4.4 to 5 GHz 5G band, and 5G Wi-Fi's 5.15 to 5.85 GHz band. Modern wireless communication system advancements have led to enormous demand for microwave devices with multifunctional features like multiband operation. A tunable and reconfigurable filter is a widely investigated because it is an essential part that effectively satisfies the criteria of multiband operation. BPFs can be designed using various techniques, including multi-layer circuits, connected structures, and balancing circuits. A dual-band BPF using a SIW was disclosed in [1]. For WLAN applications, a hybrid structure microstrip dual-band BPF was designed with -30 dB suppression level [2]. This BPF's dimensions and complex structure are undesired features. Stepped impedance transmission lines and PIN diodes have been utilised to obtain the second passband [3]. Short and open-ended stubs were used to design a dual band BPF [4]. These BPFs' size is appropriate, but their large passband insertion losses make them unsuitable for the X-band and Ku-band. BPFs with substantial S_{11} in passbands were designed using a rectangular waveguide structure [5]. A triple-layer BPF employing $\lambda/4$ UIRs was described in [6], wherein physical characteristics were used to modify the stopband. This arrangement also has a significant S_{21} in the passband and complicated geometry. In [7], another BPF with a conductor-backed SIW was designed. This filter has tunable passband frequencies; however, its large size and S_{21} in passbands are the disadvantages. In [8], new architectures made of coupled stubs were studied, and these circuits were analysed using an LC model. Combining U-shaped structures and T-shaped structures on the ground plane with coupled resonators produced a dual-layer balancing BPF with substantial return loss in passbands [9]. [10, 11] present the design of a bandpass filter for RF/microwave applications with high isolation by utilising microstrip transmission lines. [12] presents the design of a compact bandpass filter using stub loaded stepped impedance resonators, and the major drawback is that the filter offers a narrow bandwidth. In [13], a dual-layer BPF for WLAN networks was designed with stepped impedance resonators. Despite having a complicated construction, this filter performed well, with practical frequencies and high return losses in passbands. A tunable BPF with a high/low impedance structure was shown in [14], with input and output ports connected to the fundamental structure. With a -10 dB level taken into consideration, this filter's stopband rejection width is narrow, and it only suppresses up to the second harmonic. In [15], a dual band BPF was designed by using hexagon-shaped resonators and a Y-shaped high/low impedance resonator. The circuit's drawbacks include low suppression in the stopband area and substantial insertion losses in the passbands. In [16], a stepped-impedance structure-based circular BPF was introduced. This filter's physical size can be altered to change the passband positions. To achieve dual-band BPF, an asymmetrical architecture was designed in [17] employing bent feeding lines and high/low impedance stubs. It has a big size and sub-

* Corresponding author: Surendra B. Velagaleti (surendrababuvelagaleti@gmail.com).

TABLE 1. Geometric parameters of the proposed BPF.

Parameter	Values (mm)
Substrate Length (L_1)	40
Substrate Width (W_1)	40
Length of the resonator (L_2)	2
Width of the resonator (W_2)	16
Length of the resonator (L_3)	0.5
Width of the resonator (W_3)	4
Width of the resonator (W_4)	11
Width of the resonator (W_5)	6
Width of the resonator (W_6)	2.5
Width of the resonator (W_7)	5.5
Radius of the circle (r_1)	2
Radius of the circle (r_2)	1.8

stantial passband insertion losses. A reconfigurable BPF was constructed in [18] to function at WLAN frequencies. Tunable BPF has been designed by utilising semicircular resonators and symmetrical coupled structures, and the major drawback of this filter is narrow stopband and large insertion loss in the passband. The bent structures in [19] that lack a distinct transition band and small size were used to develop the BPFs. A basic BPF operating at 1.78 and 2.1 GHz frequencies, based on a high/low impedance construction, was introduced in [20]. Despite the relatively large circuit size, two high/low impedance resonators were also utilised to form the second passband. In order to construct the second passband, a symmetrical BPF has been utilised [21]. A small folded stepped-impedance resonator was chosen for this purpose. However, slow transition-bands are this filter's most notable drawback. The BPFs reported in [22–23] often have narrow stopbands. [24–27] present the design of bandpass filters by using different types of resonators, and the drawback of these filters is that they are not compact. The BPFs presented in [28–30] employed large substrates and offered narrow bandwidth with low isolation.

In this paper, a reconfigurable dual-band/single band BPF utilising a semi-circular cavity and coupled feeding lines is simulated, fabricated, and analysed. The response of the filter is controlled by varying the physical dimensions. Ansys HFSS v13 has been utilised in simulating the filter. The tunable BPF is fabricated on a 1.6 mm thickness FR-4 epoxy with material characteristics having γ_r of 4.4 and δ of 0.02. Chemical etching has been used in fabricating the filter, and the tunable BPF is measured by utilising VNA. Section-2 contains the design and analysis of a reconfigurable BPF, by utilizing PIN diodes. Section-3 contains the parametric analysis, as well as the results and discussions, and the paper is concluded with Section-4.

2. DESIGN AND ANALYSIS

2.1. Tunable BPF

The proposed tunable BPF is made of FR4 epoxy material, having ε_r of 4.4, δ of 0.02, and thickness of 1.6 mm. The tunable BPF occupies an area of $40 \times 40 \times 1.6\,\text{mm}^3$, and Figure 2 presents the photograph of the tunable BPF, and the fabrication of the filter is obtained by using chemical etching. The proposed tunable BPF is simulated by using HFSSv13. The design comprises two circular rings, and two circles are subtracted to form a trapezoidal pattern. A circular slot is incorporated in the middle trapezoidal portion of the filter. Due to the implementation of capacitive slots, the electric fields are distributed, and the intensity of electric field is also enhanced. The semicircular cavity filter selectively passes or reject certain frequencies in communication devices. The proposed tunable BPF combines the characteristics of cavity and resonator filter, which is open to transmission. This filter design consists of several key components, including a trapezoidal stub that is loaded with circular slot. To simulate its electromagnetic behaviour, the electromagnetic simulator tool is employed. The mathematical formula utilized in designing the proposed bandpass filter has been mentioned below. The dimensions that are utilized in designing the bandpass filter are mentioned in Table 1.

$$W = \frac{V_o}{2F_r}\sqrt{\frac{2}{\varepsilon_r + 1}} \tag{1}$$

where v_0 is the velocity of light in free space.

$$L = \frac{C}{2F_r\sqrt{\varepsilon_{reff}}} - 2\Delta l \tag{2}$$

$$\Delta l = 0.412h\frac{(\varepsilon_{reff} + 0.03)\,(w + 0.26h)}{(\varepsilon_{reff} - 0.258)\,(w + 0.8h)} \tag{3}$$

where Δl is the extension length

$$\varepsilon_{reff} = \frac{\varepsilon_r + 1}{2} + \frac{\varepsilon_r - 1}{2}\left[1 + \left[\frac{12h}{w}\right]\right]^{-1/2} \tag{4}$$

$$a = \frac{F}{\sqrt{1 + \frac{2h}{\Pi\varepsilon_r}\left[\ln\left(\frac{\Pi f}{2h}\right) + 1.7726\right]}} \tag{5}$$

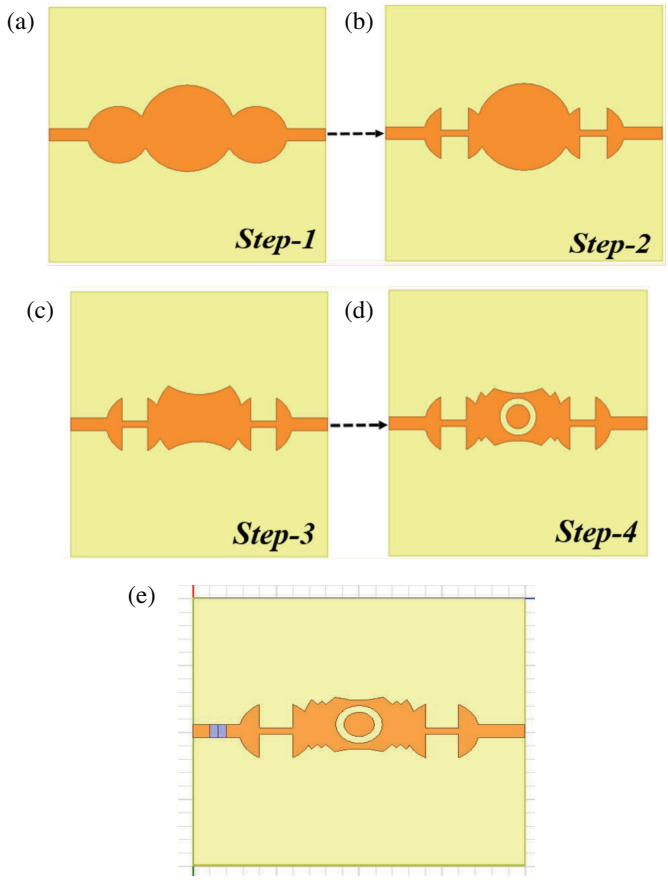

FIGURE 1. Evolution of the tunable BPF (a) Step-1, (b) Step-2, (c) Step-3, (d) Step-4 and (e) Step-5.

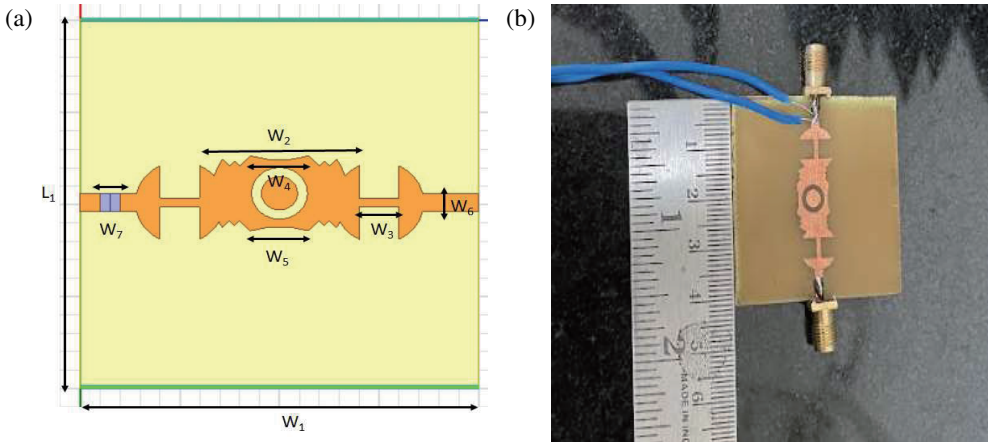

FIGURE 2. Tunable BPF. (a) Simulated design. (b) Photograph.

where $F = \frac{8.791*10^9}{f_r\sqrt{\varepsilon_r}}$ in which F_r is the resonant frequency; ε_r is the relative permittivity of the substrate; ε_{ref} is the effective relative permittivity of the substrate; h is the thickness of the substrate; L and W are length and width of the substrate; and a is the radius of the substrate. Figure 1 represents the iteration based design of a tunable BPF. In the first step, three circular stubs are fully loaded on top of the substrate. The filter produces no response within the frequency band. Step 2 is obtained by etching two rectangular strips from the circular stubs to form a semicircular cavity on both sides of the filter. In Step 3, a filter is obtained by subtracting two circular rings from the middle circular resonator. In Step 4, a diagonal square is etched from the main circular stub on the four ends. Besides, a circular slot is also etched from the main stub. Finally, in Step 5 the other two diagonal square stubs are etched from the main stub. The major purpose of the bandpass filter is to enhance selectivity and to achieve lower insertion loss, isolating chan-

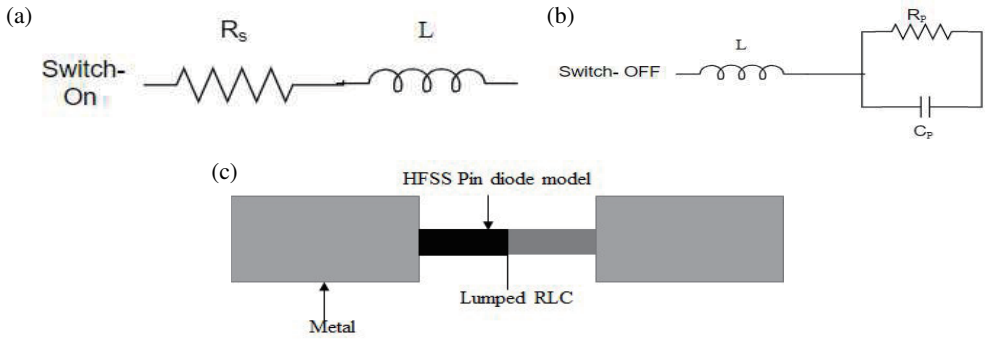

FIGURE 3. HSCH 3486 PIN diode. (a) Diode ON condition. (b) Diode OFF condition. (c) HFSS model.

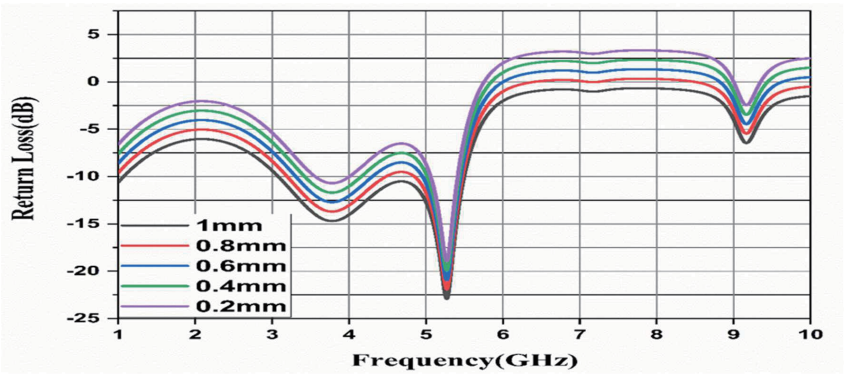

FIGURE 4. Tunable BPF's parametric analysis by varying length (Diode ON).

nels, and separating frequency bands in wireless communication. Filtering out undesired frequencies using BPFs results in an improvement in the signal-to-noise ratio, thereby enhancing the overall quality of both transmitted and received signals.

2.2. Analysis of PIN Diode

Applications for PIN diodes range from microwave frequencies to ultrahigh frequencies. Its bias current directly controls its frequency like a variable resistor in radiofrequency and microwaves [11]. Microwave PIN diode is a perfect component for the use in compact, broadband RF signal control circuits because of its small physical size in relation to its wavelength, high switching speed, and low packaging parasitic reactance. Furthermore, PIN diode can regulate high amounts of RF signal strength with substantially lower control power [12]. With less power management, PIN diode can regulate strong RF signals. Insertion loss (forward biassed) is caused by the low resistance R_s of the equivalent circuit when it is in the ON state. The equivalent circuit employs reverse bias resistance (R_P) and total capacitance (C_p) in parallel while a PIN diode is in its OFF state. The data sheets that the manufacturers supply for each PIN diode contain all of the values required for the circuit models. Figure 3 illustrates how the PIN diode is utilised in HFSS using lumped RLC boundary conditions. The first part is L, and the second part is either Rs for the ON state or a shunt combination of R_p and C_p for the OFF state. To provide a high level of frequency band reconfiguration dependability, these diodes are used.

HSCH 3486 PIN diode has been utilised to obtain the reconfigurability of the filter. According to the manufacturer's data sheet, the RLC boundary values of the diodes in HFSS during the ON state are $L = 0.3\,\text{nH}$ and $R_s = 20\,\Omega$, and during the OFF state the RLC values are $R_p = 244\,\Omega$ and $C_p = 0.01\,\text{pF}$.

3. RESULTS & DISCUSSIONS

Return loss is the front-end parameter that is to be measured for any RF device. The parametric analysis of the tunable BPF is shown in Figures 4 and 5, where the length of the lumped RLC values is varied to represent the diode's ON and OFF states. By changing the length and width of the lumped element in the design, a significant reflection coefficient has been obtained at the resonant frequency of 3 GHz–5.4 GHz (Diode ON) and 6.7 GHz (5.8 GHz–7.8 GHz) with return losses of -22 dB and -31 dB. Insertion loss is one of the important parameters that is to be measured for a microwave filter, and it should be less than 3 dB for any microwave filter. The insertion loss parametric analysis of the tunable BPF is shown in Figures 6 and 7, where the length of the lumped RLCs during the diode's ON and OFF conditions is varied. By changing their length, a significant insertion loss has been obtained at the resonant frequency of 3 GHz–5.4 GHz (Diode ON) and 6.7 GHz (5.8 GHz–7.8 GHz) with insertion losses of -1.5 dB and -2 dB.

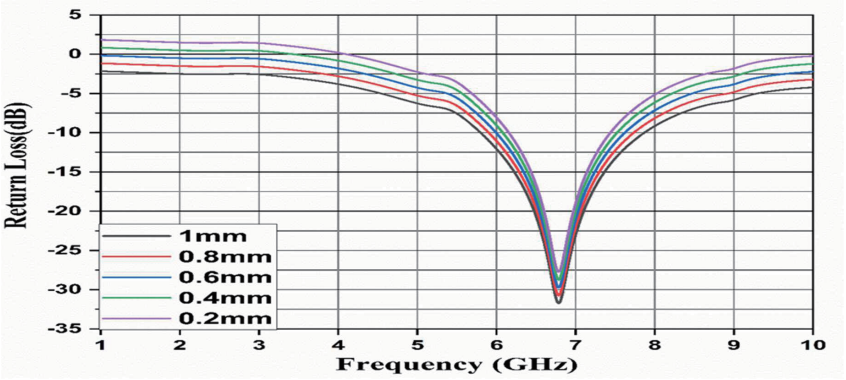

FIGURE 5. Tunable BPF's parametric analysis by varying length (Diode OFF).

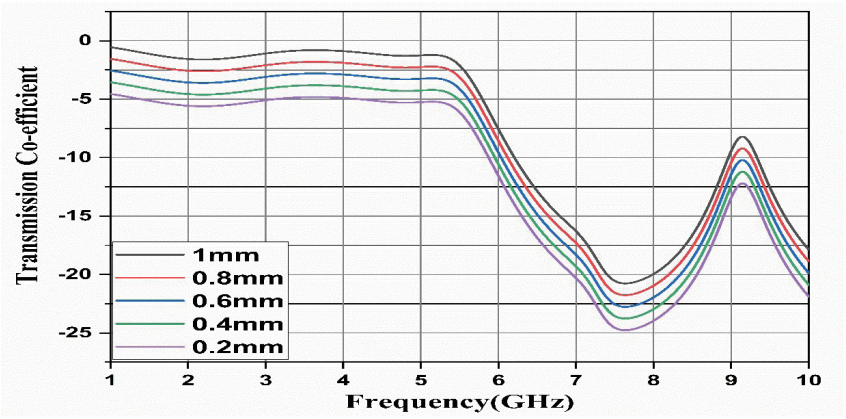

FIGURE 6. Tunable BPF's parametric analysis by varying length (Diode ON).

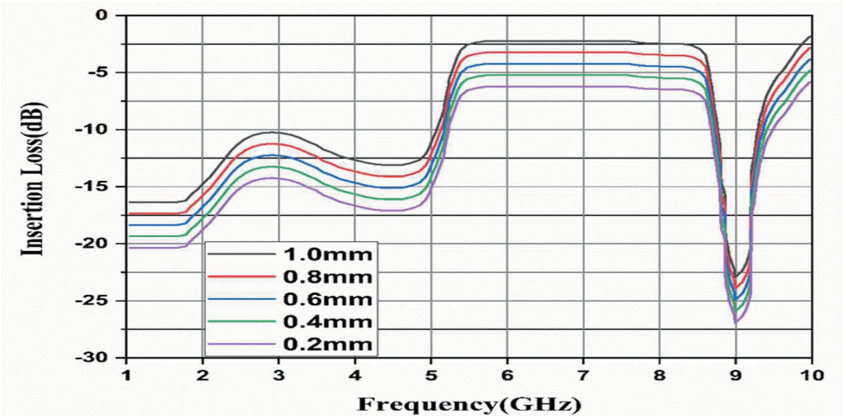

FIGURE 7. Tunable BPF's parametric analysis by varying length (Diode OFF).

Figure 8 indicates the S_{11} of the tunable BPF during the ON and OFF conditions of the diode. The return loss at both the resonating frequencies is less than -10 dB. In fact, it is even less than -10 dB, and the transmission coefficient is less than 3 dB at both the resonant frequencies as represented in Figure 8. The tunable BPF resonates at 3.7 GHz and 5.2 GHz when the diode is turned ON, and it offers an impedance bandwidth of 2.4 GHz, return losses of -15 dB, -22 dB, and insertion losses of -1.5 dB, 2 dB.

Figure 9 presents the simulated and measured S_{21} of the tunable BPF. When the diode is turned ON, the tunable BPF resonates at 3.7 GHz and 5.2 GHz and satisfies the requirement of n77 (3300–4200 MHz), n78 (3300–3800 MHz), and n79 (4400–5000 MHz) 5G applications. When the diode is turned OFF, the tunable BPF resonates at 6.7 GHz and satisfies the requirement of X-band satellite communication applications. The tunable BPF functions as a narrow band frequency tunable BPF at 6.7 GHz and offers an impedance bandwidth of

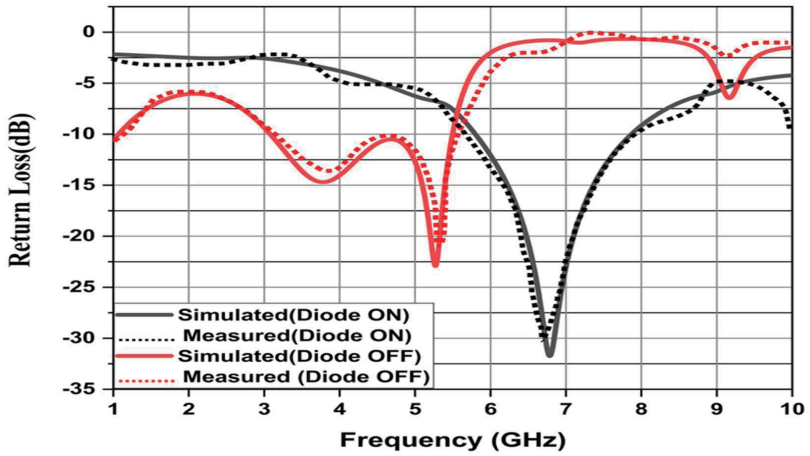

FIGURE 8. S_{11} of the tunable BPF during ON and OFF conditions of the diode.

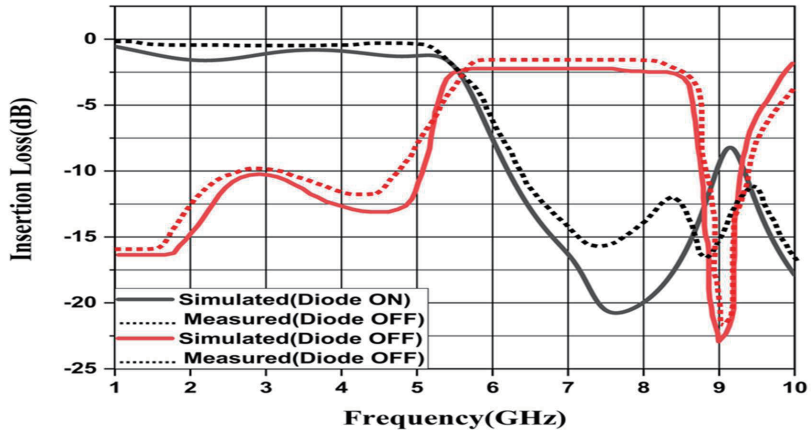

FIGURE 9. Simulated and measured S_{21} of the tunable BPF during diode ON and OFF conditions.

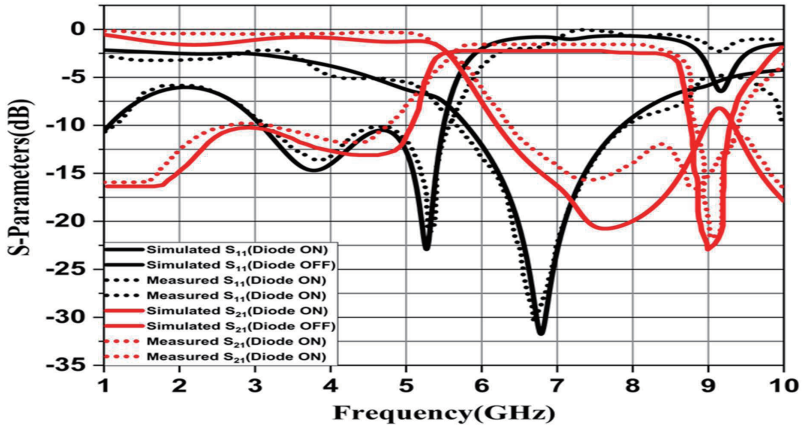

FIGURE 10. Simulated and measured S-parameters of the tunable BPF during diode ON and OFF conditions.

2 GHz, a reflection coefficient of -22 dB, and a transmission coefficient of -2 dB, which is suitable for satellite communication applications.

Figure 10 presents the S-parameters of the tunable BPF during the ON and OFF conditions of the diode. The tunable BPF resonates at 3.7 GHz and 5.2 GHz with return losses of -15 dB, -22 dB and insertion losses of -1.5 dB, 2 dB during the diode ON condition. The tunable BPF resonates at 6.7 GHz with a reflection coefficient of -22 dB and an insertion loss of -2 dB during the diode OFF condition. Figure 11 shows the time domain properties of the tunable BPF, which are computed using the group delay. The delay obtained by the filter is consistent,

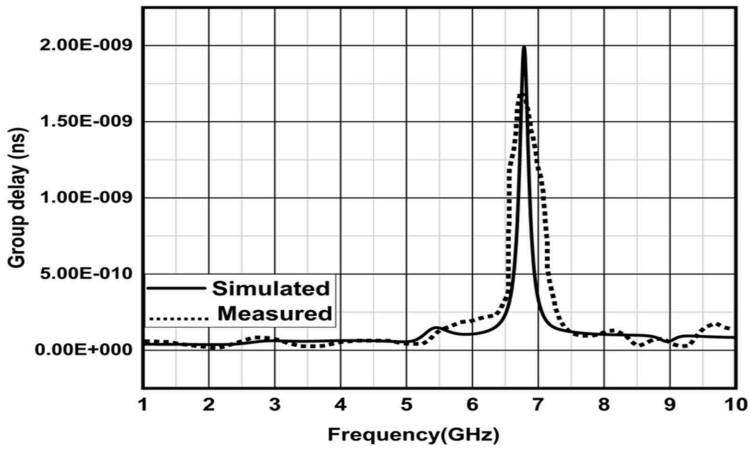

FIGURE 11. Group delay of the tunable BPF during diode OFF condition.

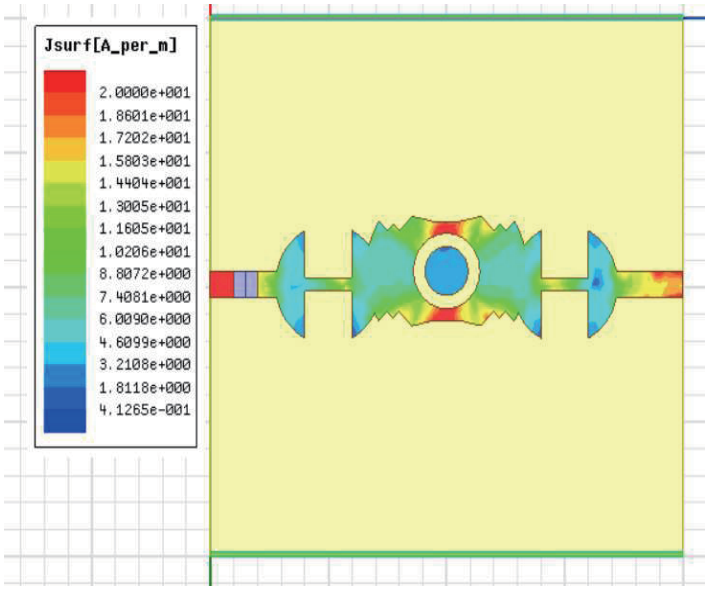

FIGURE 12. Surface current distribution of the tunable BPF.

TABLE 2. Comparison of the tunable BPF with the other tunable BPF's available in the literature.

References	F(GHz)	FBW	IL (dB)	RL (dB)	Group Delay (nS)	Size (λ_g^2)
[1]	3.5/5.24	—	1.5/1.6	12/13	—	1.4×1.4
[2]	2.55/3.65	6.72/5.45	1.2/2	19/19	0.9	0.89×0.89
[3]	2.49/3.50	15.60/8	1.22/1.22	13/13	0.4	0.87×0.87
[4]	2.53/5.76	4/3	1.3/1.4	15/14	0.963	1.5×1.7
[5]	2/4	5.5/4	1.22/1.23	17/17	0.879	1.2×1.32
[6]	2.4/3.8	12/10	2/1	18/19	0.756	0.87×0.87
[7]	2.5/1.3	2/0.9	0.99/0.55	17/19	0.854	0.68×0.68
[8]	2.5/5.6	—	0.58/1.8	16/15	—	0.258×0.258
[9]	2.1/2.6	1.4/2.1	1.9/1.63	15/19	0.778	0.798×0.798
This study	3.7, 5.2/6.7	2.4/2	−1.5, −2/−2	−15, −22/−31	0.2/0.2	0.188×0.188

resulting in minimal signal distortion, and offers a group delay 2 nS for the simulated and 1.7 nS for the measured filter. Figure 12 presents the surface current distribution of the tunable BPF, which shows the signal transmission across the semicircular cavities

The performance of the tunable BPF in this article is compared with that of several other tunable BPFs stated in Table 2. It is demonstrated that our filters outperform the filters in the references at the same size level in terms of insertion and return losses. Moreover, the insertion losses continue to be the lowest among the equivalents. It is evident from a comparison of the results that this tunable bandpass filter has superior bandwidth and insertion loss.

4. CONCLUSION

This work contains a unique tunable BPF made up of a semicircular cavity that can reconfigure the frequency. The tunable BPF is made up of a semicircular cavity and a circular ring that are scalable and reproducible. The prototype is inexpensive, small, and is capable of doing several operations. This tunable BPF handles the issues of dynamic spectrum access, efficient spectrum usage, bandwidth management, and many more wireless communication applications. The tunable BPF is designed for high band rejection, steep passband edges, and low insertion loss. The proposed tunable BPF is suitable for n77 (3300–4200 MHz), n78 (3300–3800 MHz), and n79 (4400–5000 MHz) 5G applications and X-band satellite communication applications.

REFERENCES

[1] Li, P., H. Chu, D. Zhao, and R. S. Chen, "Compact dual-band balanced SIW bandpass filter with improved common-mode suppression," *IEEE Microwave and Wireless Components Letters*, Vol. 27, No. 4, 347–349, Apr. 2017.

[2] Ieu, W., D. Zhang, and D. Zhou, "High-selectivity dual-mode dual-band microstrip bandpass filter with multi-transmission zeros," *Electronics Letters*, Vol. 53, No. 7, 482–484, Mar. 2017.

[3] Zhu, H. and A. M. Abbosh, "Single-and dual-band bandpass filters using coupled stepped-impedance resonators with embedded coupled-lines," *IEEE Microwave and Wireless Components Letters*, Vol. 26, No. 9, 675–677, Sep. 2016.

[4] Zhang, Z.-C., Q.-X. Chu, and F.-C. Chen, "Compact dual-band bandpass filters using open-/short-circuited stub-loaded λ/4 resonators," *IEEE Microwave and Wireless Components Letters*, Vol. 25, No. 10, 657–659, Oct. 2015.

[5] Zhou, K., C.-X. Zhou, and W. Wu, "Resonance characteristics of substrate-integrated rectangular cavity and their applications to dual-band and wide-stopband bandpass filters design," *IEEE Transactions on Microwave Theory and Techniques*, Vol. 65, No. 5, 1511–1524, May 2017.

[6] Li, Y.-L., J.-X. Chen, Q.-Y. Lu, W. Qin, W. Li, and Z.-H. Bao, "A new and simple design approach for harmonic suppression in bandpass filter," *IEEE Microwave and Wireless Components Letters*, Vol. 27, No. 2, 126–128, Feb. 2017.

[7] Xiao, J.-K., M. Zhu, J.-G. Ma, and J.-S. Hong, "Conductor-backed CPW bandpass filters with electromagnetic couplings," *IEEE Microwave and Wireless Components Letters*, Vol. 26, No. 6, 401–403, Jun. 2016.

[8] Shen, G., W. Che, W. Feng, and Q. Xue, "Analytical design of compact dual-band filters using dual composite right-/left-handed resonators," *IEEE Transactions on Microwave Theory and Techniques*, Vol. 65, No. 3, 804–814, Mar. 2017.

[9] Bagci, F., A. Fernández-Prieto, A. Lujambio, J. Martel, J. Bernal, and F. Medina, "Compact balanced dual-band bandpass filter based on modified coupled-embedded resonators," *IEEE Microwave and Wireless Components Letters*, Vol. 27, No. 1, 31–33, Jan. 2017.

[10] Hong, J.-S. G. and M. J. Lancaster, *Microstrip Filters for RF/Microwave Applications*, John Wiley & Sons, 2004.

[11] Chang, Y., W. Feng, and W. Che, "Dual-band bandpass filters with high isolation using coupled lines," *International Journal of Electronics*, Vol. 103, No. 3, 372–383, Mar. 2016.

[12] Denis, B., K. Song, and F. Zhang, "Compact dual-band bandpass filter using open stub-loaded stepped impedance resonator with cross-slots," *International Journal of Microwave and Wireless Technologies*, Vol. 9, No. 2, 269–274, Mar. 2017.

[13] Song, K., T. Pan, and Y. Fan, "Dual-band bandpass filter based on mixed electric and magnetic coupling of the hybrid quasi-lumped resonator," *International Journal of Electronics*, Vol. 101, No. 8, 1096–1105, Aug. 2014.

[14] Kim, C., T. H. Lee, B. Shrestha, and K. C. Son, "Miniaturized dual-band bandpass filter based on stepped impedance resonators," *Microwave and Optical Technology Letters*, Vol. 59, No. 5, 1116–1119, May 2017.

[15] Tang, M.-C., T. Shi, S. Chen, H. Xiong, and X. Zeng, "A compact triple-mode filter with Y-type stepped-impedance stub (Y-SIS) for PCS and WiMAX applications," *Wireless Personal Communications*, Vol. 94, No. 3, 1331–1339, 2017.

[16] Wang, W., Q. Cao, C. Yang, Y. Wang, and Y. Chen, "Design of dual-bandpass filters using stepped-impedance circular ring resonator," *Electronics Letters*, Vol. 51, No. 25, 2117–2119, Dec. 2015.

[17] Pal, M., R. Ghatak, and P. Sarkar, "Compact dual-band bandpass filter using asymmetric stepped impedance stub loaded multimode resonator," *International Journal of Microwave and Wireless Technologies*, Vol. 9, No. 1, 45–50, 2017.

[18] Xu, L.-J., G. Zhang, Y.-M. Tang, and Y.-M. Bo, "Compact dual-mode dual-band bandpass filter with wide stopband for WLAN applications," *Electronics Letters*, Vol. 51, No. 17, 1372–1374, Aug. 2015.

[19] Navya, A., G. Immadi, and M. V. Narayana, "Design and analysis of a compact wide-band BPF using quarter wave transmission lines," *Journal of Engineering Science & Technology Review*, Vol. 15, No. 4, 33–36, 2022.

[20] ——, "Flexible ku/k band frequency reconfigurable bandpass filter," *AIMS Electronics and Electrical Engineering*, Vol. 6, No. 1, 16–28, 2022.

[21] Ambati, N., G. Immadi, M. V. Narayana, K. R. Bareddy, M. S. Prapurna, and J. Yanapu, "Parametric analysis of the defected ground structure-based hairpin band pass filter for VSAT system on chip applications," *Engineering, Technology & Applied Science Research*, Vol. 11, No. 6, 7892–7896, Dec. 2021.

[22] Navya, A., G. Immadi, and M. V. Narayana, "A low-profile wideband BPF for ku band applications," *Progress In Electromagnetics Research Letters*, Vol. 100, 127–135, 2021.

[23] Immadi, G., N. K. Majji, M. V. Narayana, and A. Navya, "Comparative analysis of pass band characteristics of a rectangular waveguide with and without a dielectric slab," *International Journal of Innovative Technology and Exploring Engineering*, Vol. 8, No. 6, 1209–1211, 2019.

[24] Immadi, G., M. V. Narayana, A. Navya, Y. D. S. Sairam, and K. Shrimanth, "Design and analysis of micro strip circular ring band stop filter," *International Journal of Engineering and Advanced Technology*, Vol. 8, No. 4, 788–790, 2019.

[25] Lin, L., P.-P. Xu, J.-L. Liu, B. Wu, T. Su, and C.-H. Liang, "Dual-band bandpass filters using a novel quad-mode stub-loaded ring resonator," *Progress In Electromagnetics Research Letters*, Vol. 55, 31–38, 2015.

[26] Li, D., Y. Zhang, K. Song, K. Xu, and J. L.-W. Li, "Miniaturized close dual-band bandpass filter based on short stub-loaded stepped-impedance resonators," *Electromagnetics*, Vol. 35, No. 1, 49–58, 2015.

[27] Lu, D., N. S. Barker, and X.-H. Tang, "Miniaturized dual-band filter with return loss bandwidth and transmission zero control," *International Journal of Microwave and Wireless Technologies*, Vol. 9, No. 7, 1459–1465, 2017.

[28] Hammed, R. T., "Miniaturized dual-band bandpass filter using E-shape microstrip structure," *AEU — International Journal of Electronics and Communications*, Vol. 69, No. 11, 1667–1671, 2015.

[29] Song, K., F. Zhang, and Y. Fan, "Miniaturized dual-band bandpass filter with good frequency selectivity using SIR and DGS," *AEU — International Journal of Electronics and Communications*, Vol. 68, No. 5, 384–387, 2014.

[30] Navya, A., G. Immadi, M. V. Narayana, and A. S. Madhuri, "Design and analysis of a quad band BPF using ring resonator," in *2023 7th International Conference on Computation System and Information Technology for Sustainable Solutions (CSITSS)*, 1–4, 2023.